

NONLINEAR ANALYSIS OF CONVECTIVE INSTABILITIES IN HEATED CYLINDRICAL CAVITIES

¹R. Touihri, ²A. El Gallaf, ²D. Henry & ²H. BenHadid

¹LAMSIN-ENIT, BP 37 Tunis le Bélvédère 1002 Tunis, Tunisie.

²LMFA/ECL, 36 Av. Guy de Collongue, 69134 Ecully Cedex France

E-mail : ridha.touihri@ipeim.rnu.tn

We consider a cylindrical cavity heated from below, with a free surface at the top. This configuration corresponds to the well known Rayleigh-Marangoni-Bénard situation. The results of the stability study are given through a stability diagrams giving the evolution of the primary thresholds Ra_c as a function of the Biot number Bi , the Marangoni number Ma , and the aspect ratio of the cavity $A = R/H$ (where R is the radius of the cavity and H is its height). The nonlinear evolution of the convection beyond its onset is given by a bifurcation diagrams giving the evolution of the Nusselt number or the vertical velocity in one point in the cavity, versus the Grashof number Gr .

1 INTRODUCTION

The onset of thermo-convective instabilities in fluid layer heated from below with free surface at the top is a classical problem in fluid Mechanics. The bibliography on this subject is very rich, we can cite two interesting reviews given by the books of Koschmider [1] and Dijkstra [2]. For this configuration, it is well known that the convection sets on when the temperature difference becomes larger than a certain critical value. This instability is due to two different effects. The first is due to the gravity force, and was introduced first by the experiments of Bénard [3] and studied theoretically by Rayleigh [4]. Thus, it is referred to as Rayleigh-Bénard effect. The second possible cause of this instability, is the so-called Marangoni effect, which is due to the capillary forces appearing at the free surface whose tension is a function of temperature (Pearson [5]). Both effects combine and give rise to 'Bénard-Marangoni' instability studied in 1964 by Nield [6].

Experimentally, we can cite the work of Koschmider and Prahl [7], and more recently, Johnson and Narayanan [8]. For the cylindrical geometry we consider here, Vrentas et al. [9] made a linear axisymmetric approach and compared his results with Charlson and Sani [10] for the buoyancy-driven convection in a rigid-wall cylinder with an insulating side wall. These two latter works are in good agreement with the nonlinear study made by Wagner et al. [11]. Dauby et al. [12], made a numerical linear study by using a spectral method with chebychev decomposition. Their code allows to calculate altogether the critical values of Marangoni and Rayleigh numbers. They found some difference with Vrentas et al. [9] for $A = 1$. Recently Assemat and Bergeon [13] studied the effect of changing the container shape, from circular to elliptical, on the pattern formation in Marangoni convection for small aspect ratio containers.

In this paper, we consider a cylindrical cavity heated from below, with a free surface at the top. We solve the Navier-Stokes equation coupled with the energy one. To study the nonlinear evolution of the convection beyond its onset, we developed an appropriate continuation method. This method is extended to the calculation of the primary thresholds.

Our purpose is to study the effect of the free surface and the tension surface at the top added to the pure thermal rigid wall configuration we studied before (Touihri et al.

[14]). So we will calculate a stability diagrams giving the critical Rayleigh number Ra_c , corresponding to the onset of the convection, as a function of the aspect ratio of the cavity, for some values of the Marangni number Ma and the Biot number Bi . Some of this critical values are compared with the literature. The results of the nonlinear evolution of the convection beyond its onset are given through a bifurcation diagrams for some values of A , Pr , Ma , and Bi .

2 PHYSICAL MODEL

We consider an incompressible newtonian fluid confined in a vertical cylindrical cavity of aspect ratio $A = R/H$ where H is the height and R the Radius. The lower end of the cylinder is assumed isothermal and held at temperature T_h , which is greater than the temperature T_c of the free surface at the top, and the sidewalls are considered to be adiabatic. All the physical characteristics are taken as constant, except the density which varies linearly with temperature in the buoyancy term, $\rho = \rho_0(1 - \beta(T - T_0))$ (Boussinesq approximation), where β is the thermal expansion coefficient and T_0 the mean temperature, $T_0 = (T_h + T_c)/2$.

The governing equations for the temperature T , the pressure p and the velocity \mathbf{u} are the Navier-Stokes equations coupled with the energy equation. By scaling length by the height H of the cylinder, time by H^2/ν , velocity by $U_{ref} = \nu Gr/H$, and by introducing the dimensionless temperature field $\theta = (T - T_0)/(T_h - T_c)$, the equations can be written in their dimensionless form as:

$$\frac{\partial \mathbf{u}}{\partial t} = -(\mathbf{u} \cdot \nabla) \mathbf{u} - \nabla p + \nabla^2 \mathbf{u} + Gr \theta \hat{z} \quad (1)$$

$$\nabla \cdot \mathbf{u} = 0, \quad (2)$$

$$\frac{\partial \theta}{\partial t} = Gr \mathbf{u} \cdot \nabla \theta + \frac{1}{Pr} \cdot \nabla^2 \theta, \quad (3)$$

where $Gr = (g\beta(T_h - T_c)H^3)/\nu^2$, and $Pr = \nu/\kappa$ are respectively the Grashof and the Prandtl numbers. We can also define the Rayleigh number as $Ra = Gr.Pr$. In these relations, κ is the thermal diffusivity and ν the kinematic viscosity.

For the boundary conditions, except the free surface, the no-slip velocity boundary condition is prescribed at all the container walls, the temperature is fixed at the the bottom, and along the lateral wall ($r = a$), the normal heat flux is zero. For the free surface at the top, the fluid is assumed to be plane and nondeformable. The surface tension σ is supposed to be a linear function of the temperature, so we define γ as $\gamma = \partial\sigma/\partial T$.

We assume also, that the heat is transferred from liquid to the ambient gas according to Newton's law of cooling, which introduce the Biot number. Therefore, in their dimensionless form, the boundary conditions can be written as follows:

$$\text{at } r = A, \quad u = v = w = 0, \quad \frac{\partial \theta}{\partial n} = 0, \quad (4)$$

$$\text{at } z = 0, \quad u = v = w = 0, \quad \theta = 1, \quad (5)$$

$$\text{at } z = 1, \quad \frac{\partial u}{\partial z} = Ma \frac{\partial \theta}{\partial x}, \frac{\partial v}{\partial z} = Ma \frac{\partial \theta}{\partial y}, w = 0 \quad \frac{\partial \theta}{\partial z} = -Bi\theta - 1, \quad (6)$$

where $Bi = h * H/\lambda$ is the Biot number, and $Ma = \gamma(T_h - T_g)H/\rho\kappa\nu$ is the Marangoni number.

Setting $\mathbf{u} = \mathbf{0}$, we obtain the temperature profile of the static solution, $\theta(z) = 1 - z$ which corresponds to the diffusive regime.

3 RESULTS

3.1 Validation

In this section we compare our results giving the critical values Ra_c , corresponding to the three first modes, with some values given by the literature. Our results are obtained by using both the spectral element method (SEM) and finite element method (FEM). The critical values given by the literature corresponds to the axisymmetric mode ($m = 0$), which is not the first mode for the given cases. From tables (1) and (2), we can easily remark that our values are in good agreement with Dauby et al. [12].

Mode	SEM	FEM	Dauby et al. [12]	Vrentas et al. [9]
$m = 1$	1101.93	1118.86	-	-
$m = 0$	1463.34	1500.90	1482.12	1628.2
$m = 2$	1481.84	-	-	-

Table 1: Comparison of our results with some given by the literature : critical values Ra_c for the first modes, for $A = 1$, $Ma = 0$ and $Bi = 1$.

Mode	SEM	FEM	Dauby et al. [12]	Vrentas et al. [9]
$m = 1$	951.19	960.45	-	-
$m = 2$	1374.95	-	-	-
$m = 0$	1425.82	-	1426.24	1565.9

Table 2: Comparison of our results with some given by the literature : critical values Ra_c for the first modes, for $A = 1$, $Ma = 0$ and $Bi = 0.1$.

3.2 Onset of the convection

3.2.1 Effect of the aspect ratio

The stability diagrams given in Fig. (1.a) and Fig. (1.b) show the evolution of the three first primary thersholds correponding to the modes $m = 0$, $m = 1$, and $m = 2$, as a function of the aspect ratio A , respectively for ($Bi = 100$ and $Ma = 0$) and ($Bi = 1$ and $Ma = 100$). These resulsrts are obtained by using the Spectral element method (SEM). To compare this method with the Finite element method, we give also in the first diagram the evolution of the first critical threshold, calculated by the Finite element method. From these diagrams we notice that the convection sets in with the one roll assymmetric mode ($m = 1$) for the long ($0.5 \leq A \leq 1$) and plate ($2 \leq A \leq 2.5$) cavities, and with the axisymmetric mode for the intermediate values of A ($1 \leq A \leq 2$).

3.2.2 Effect of the biot number Bi and the Marangoni number Ma

The stability diagrams given in Fig. (2.a) and Fig. (2.b) show respectively the evolution of the critical Rayleigh numbers $Ra_{c(m=1)}$ for $A = 1$, and the first critical Rayleigh number $Ra_{c(m=0)}$ for $A = 1.5$ as a function of Bi and some values of Ma . From these diagrams, we can notice that for large values of Bi , where the heat is essentially transferred by convection, the Marangoni number Ma , has no effect on the thresholds. This can be explained by the fact that for infinite values of Bi , the boundary conditions at the top on the temperature field given by the equation (6), becomes : $T_c = T_g$ for $z = 1$. Therefore, the surface tension has no effect on the flow at the free surface. When Bi decreases the effect of Ma becomes greater. For $Bi = 0$, the model corresponds to a fixed heat flux at the top. We can notice also that there is no interaction between the modes $m = 0$ and $m = 1$ for $A = 1$, since the convection sets in with the asymmetric one roll mode for different values of Bi and Ma .

We can see also that there would be a value of the Marangoni number Ma_0 at which the effect of the surface tension at the top changes from destabilizer for $Ma < Ma_0$, to stabilizer by counterbalancing the Rayleigh-Bénard effect for $Ma > Ma_0$.

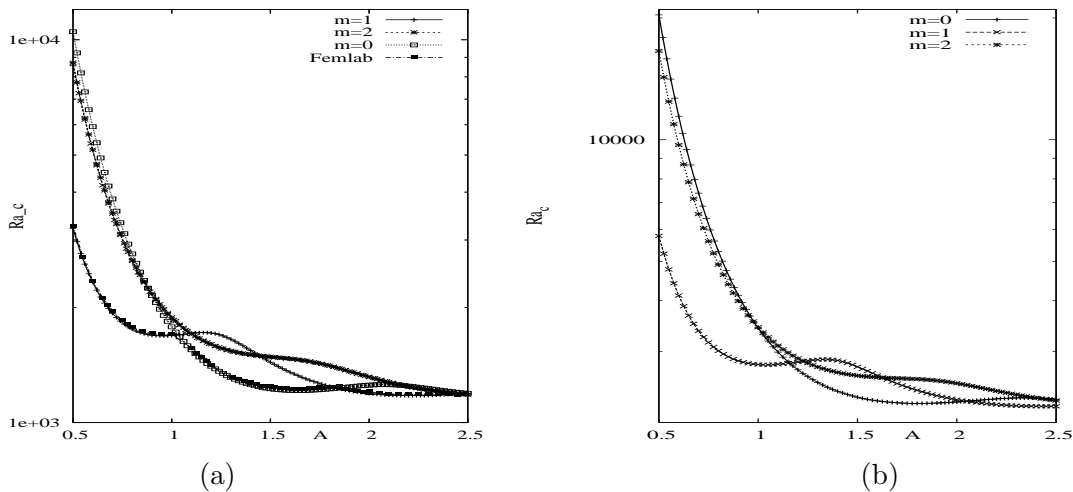


Figure 1: Evolution of the three first primary thresholds corresponding to the modes $m = 0$, $m = 1$, and $m = 2$, as a function of the aspect ratio A . (Left : $Bi = 100$ and $Ma = 0$. Right : $Bi = 1$ and $Ma = 100$).

3.3 Nonlinear evolution of the convection

The bifurcation diagram presented in Fig. (3.a) the evolution of the vertical component of the velocity as a function of the Grashof number Gr , for $A = 1.5$, $Pr = 1$, $Bi = 100$ et $Ma = 0$. As predicted by the linear analysis, the convection sets in with an axisymmetric ($m = 0$). So we obtain a first primary bifurcation point at $Ra_{c(m=0)} = 1224.75$. This mode breaks no symmetries from the static solution, so we obtain a transcritical bifurcation. To make this point clearer we give in Fig. (3.b) the evolution of Nusselt number Nu , for the axisymmetric solution, as a function of Gr , where we can see that the two halves of branches of solutions are not superposed. Beyond the onset of the convection, we obtained two secondary bifurcation points Fig. (3). The first is due to an unstable eigenvector with

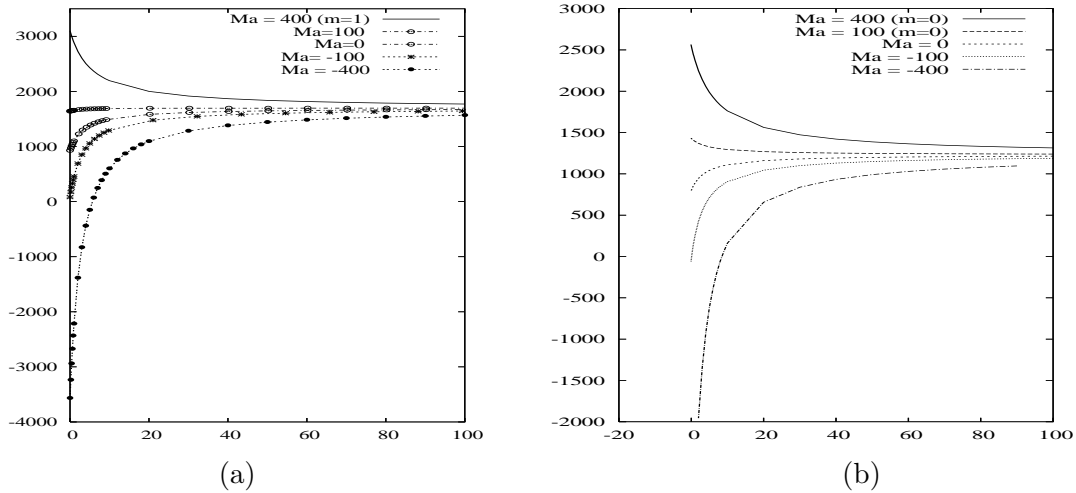


Figure 2: Evolution of first primary threshold $Ra_{c(m=1)}$ corresponding to the onset of the convection as a function of Bi , for some values of Ma . (Left : $A = 1$ and right : $A = 1.5$).

$m = 2$ mode, and appears at $Gr_{c(m=2)} = 10213.25$. The second is due to an unstable eigenvector with $m = 1$ mode, and appears at $Gr_{c(m=1)} = 12637.73$. For both cases, the bifurcations are subcritical and pitchfork, because the new stable branches break an infinite number of symmetries from either the static or the axisymmetric solution.

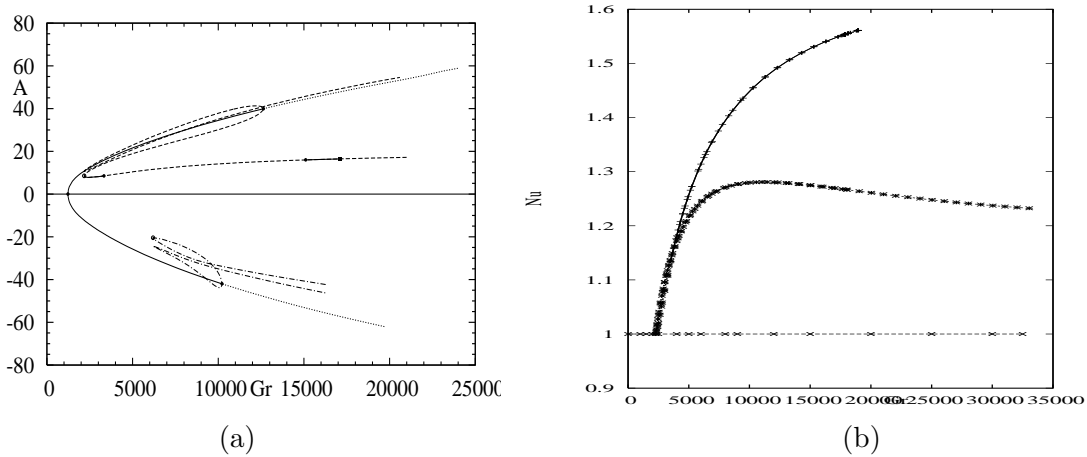


Figure 3: Bifurcation diagram for $A = 1.5$, $Pr = 1$, $Bi = 100$, $Pr = 1$ and $Ma = 0$. Left : Evolution of the vertical component of the velocity at one point in the cavity as a function of the Grashof number Gr . Right : Evolution of the Nusselt number Nu for the axisymmetric solution versus the Grashof number Gr .

4 CONCLUSION

In this work we presented a numerical simulation of a nonlinear convective instabilities Marangoni-Rayleigh-Bénard convection in cylindrical cavity. The results of the onset of

convection were presented through some stability diagrams giving the evolution of the primary thresholds as a function of the aspect ratio ($A = R/H$) and the Biot number Bi for some value of the Marangoni number Ma . It has been showed that the surface tension has no effect for large values of Bi . For small values of Bi , there would be a critical value Ma_0 , where the effect of the surface tension changes from stabilizer to distabilizer. For $A = 1.5$ we have detected a transcritical bifurcation corresponding to the axisymmetric mode ($m = 0$). Beyond the onset of the convection, we obtained two secondary bifurcation points. The first is due to an unstable eigenvector with $m = 2$ mode. The second is due to an unstable eigenvector with $m = 1$ mode. In the recent future, wa are managing to calculate some hopf bifurcation points. At these points the flow becomes insteady and oscillatory. An energetic analysis will be made to show the physical phenomena responsible on these transitions.

References

- [1] E. L. Koshmider, 'Bénard Cells and Taylor Vorices', *Cambridge University press, Cambridge, 1993*
- [2] H. A. Dijkstra, Free Surface Flows, edited by C. H. Hendrik et al. (Springer-Verlag, Wiem), CISM,Courses Lect. **391**, pp. 101-144. (1998)
- [3] H Bénard, Rev. gen. Sci. Pure Appl. **11**, 1261 (1990).
- [4] Lord Rayleigh, Philos. Mag. **32**, 529 (1916).
- [5] J. R. A. Pearson, J. Fluid Mech. **4**, 489 (1958).
- [6] D. A. Nield, J. Fluid Mech. **19**, 341 (1964).
- [7] E. L. Koshmider and S. A. Prahl, J. Fluid Mech. **215**, 571 (1990).
- [8] D. Johnson and R. Narayanan, Phys. Rev. E **54**, R3102 (1996).
- [9] J. S. Vrentas, R. Nayaranan & S. S. Agrawal, 'Free surface convection in a bounded cylindrical géometry', *Int. J. heat and mass transfer.* **24**, N9, pp. 1513-1529, (1981).
- [10] G. S. Charlson and R. L. Sani, 'Thermoconductive instability in a bounded cylindrical fluid layer, *Int. J. heat and mass transfer.* **13**, pp. 1479-1496, (1970).
- [11] C. Wagner, R. Friedrich, and R. Nayaranan, Phys. Fluids **6**, 1425 (1994).
- [12] P. C. Dauby, G. Lebon & E Bouhy, 'Linear Bénard-Marangoni instability in rigid circular containers', (*Physical Review E*, **56**, N1, pp. 520-530, 1997.)
- [13] P. Assemat and A. Bergeon, 'Nonlinear Marangoni convection in circular and elliptical cylinders', *Phys. Fluids*, **19** 104101 (2007).
- [14] R. Touihri, H. Ben Hadid, D. henry, *Phys. Fluids*, **11**, N8, pp. 2078-2088, (1999)